Rigidity index of soft remolded clays during thixotropic hardening

Jing Peng, UMass Amherst, Amherst, MA, USA, 1(413)-276-8915, jpeng@umass.edu
Don J. DeGroot, UMass Amherst, Amherst, MA, USA, degroot@umass.edu
Yiming Cao, UMass Amherst, Amherst, MA, USA, yimingcao@umass.edu
Guoping Zhang, UMass Amherst, Amherst, MA, USA, zhangg@umass.edu

ABSTRACT

This paper presents results from an experimental program that measured the thixotropic behavior of several remolded soft clays with varying plasticity. Measurements were conducted at various curing times ranging from 1.0 hour to 64 days. The undrained shear strength s_u was measured using the fall cone while companion specimens were also prepared and mounted in a bender element jig for measurement of temporal changes in shear wave velocity V_{vh}. The bender element specimens allowed for much greater frequency of repeated data collection since the measurement was nondestructive and only one specimen was needed per clay for the full curing period. Furthermore, the combination of measurements provided data at each curing period for the rigidity index I_R taken as the ratio of the small-strain shear modulus G_{max} to s_u. Values of s_u and V_{vh} increased significantly with time for all the clays, especially at a higher rate for the first 2 to 4 days. The full time-series dataset of each clay enabled the evolution of I_R during thixotropic hardening, which was found to be nearly constant over time for each of the studied clays. These data shed light on analyzing the behavior of offshore infrastructure and in situ tools that remold soft clays during installation such as pipelines, embedment anchors, and full-flow penetrometers.

Keywords: thixotropy, rigidity index, undrained shear strength, shear wave velocity

INTRODUCTION

Large-strain shearing of clays during sampling, in situ testing, and infrastructure installation often results in a loss of intact undrained shear resistance. Depending on the sensitivity of a clay, the loss of undrained shear strength after complete remolding can vary from very little for heavily overconsolidated, low sensitivity clays to near complete for high-sensitivity quick clays (Moretto, 1948; Skempton and Northey, 1952). However, it has long been observed that either partially or fully remolded clays gradually regain undrained shear strength with time even under conditions of constant composition and temperature (Mitchell, 1960; Zhang et al., 2013; Zhang et al., 2017). This phenomenon has also been observed for other materials such as clay suspensions, crude oils, paints, and coatings (Arnold and Goodeve, 1940; Chang et al., 1999; Gamble, 1936; Ma et al., 2018; Turner and Rodewald, 1949). Such a stiffness-hardening process is known as thixotropy and for soils is defined by Mitchell and Soga (2005) as "… an isothermal, reversible, time-dependent process occurring under conditions of constant composition and volume whereby a material stiffens while at rest and softens or liquefies upon remolding."

In offshore geotechnical engineering practice, thixotropic hardening after soil remolding can be a significant consideration. For example, the undrained shear strength (s_u) of clay along the soil-structure interface of a driven pile or suction caisson may decrease upon completion of installation because of the high interface shear strains. However, a progressive regain in undrained shear strength can occur during post installation due to the combined effects of consolidation and thixotropy. For some clays the regain in undrained shear strength due to thixotropy alone can be greater than a factor of 2 (Mitchell, 1960). For suction caissons, the amount of thixotropic strength gain and the required hardening time after installation are controlled by how the caisson is installed (e.g., Andersen and Jostad, 2004, 2002). Several studies have been conducted to better understand how various basic soil properties such as water content, plasticity index, activity, and clay mineralogy influence the thixotropic hardening process. For example, Yang and Andersen (2016) studied several empirical correlations and found that liquidity index and water content show the best correlation with thixotropy strength ratio (s_u after *t*-days recovery divided by the remolded s_u) and that higher thixotropic strength ratios were achieved by clays with higher water content and liquidity index. Similar experimental results were also reported by others such as Lunne and Andersen (2007) and Seng and Tanaka (2012).

The rigidity index (I_R), as proposed by Vesic (1972), is defined as the ratio of the shear modulus (G) to s_u and is a soil property frequently used as an indicator of clay stiffness. In offshore practice it is used for several applications including estimating the coefficient of consolidation from piezocone dissipation tests (Teh and Houlsby 1991), post installation consolidation of piles (Randolph 2013), modeling of piezocone partial drainage conditions during penetration (DeJong and Randolph 2012), and interpretation of full-flow penetrometer behavior (Low et al., 2010). The I_R of intact clays can be estimated from in situ tests such as the seismic piezocone (e.g., Krage et al. 2014) either alone or in combination with advanced laboratory test data such anisotropically consolidated triaxial compression (CAUC) tests conducted on high-quality samples. In the absence of such measurements, empirical correlations have been developed including that of Keaveny and Mitchell (1986) and further developed by Mayne (2007), which uses plasticity index and overconsolidation ratio to estimate I_R.

However, there is little to no data available on how I_R may differ for intact clays versus remolded clays and how I_R potentially evolves during thixotropic hardening. To this end the objective of the study presented in this paper was to investigate the thixotropic behavior of fully remolded soft clays and the evolution of I_R during thixotropic hardening. The small-strain shear modulus (G_{max}) and s_u of the tested clay samples were measured using bender elements (BEs) for G_{max} and the fall cone (FC) for s_u. The paper describes the test soils and measurement methods and a presentation and interpretation of the measured data.

TEST SOILS AND METHODS

Test Soils

Six soft clays were tested in this work including Kaolinite, PureGold Gel, Onsøy, Troll, Atchafalaya, and Boston Blue Clay (BBC). Kaolinite and PureGold Gel (a Na-montmorillonite) are manufactured clay powders obtained from The Feldspar Corporation (Edgar, Florida, USA) and CETCO (Arlington Heights, Illinois, USA), respectively. The other four are natural clays collected from different test sites: (1) Onsøy is a sensitive marine clay that was collected at the Norwegian Geotechnical Institute's (NGI) test site located in south-eastern Norway; (2) Atchafalaya clay was collected from Assumption Parish, Louisiana; (3) Troll clay was collected from the Norwegian sector of the North Sea, and (4) BBC is a glacial marine clay that was collected from Boston, Massachusetts. Table 1 presents basic soil properties, including Atterberg limits and clay fraction (CF) which were determined in accordance to ASTM (2020) except for the liquid limit test which was conducted using the fall cone method as per ISO 17892-12 (2018). Based on the Unified Soil Classification System (USCS) (ASTM, 2020), BBC and Kaolinite are classified as CL and MH, respectively, while Atchafalaya, PureGold Gel, Troll and Onsøy clays are all classified as CH. Batches of the clays for thixotropy testing were prepared to a water content at or close to the liquid limit, thoroughly mixed and left overnight in a temperature-controlled box at 24˚C for thermal equilibrium. Prior to set-up of individual thixotropy test specimens, the clays were again thoroughly remixed.

Table 1 Index and classification properties of test clays

Soil		Atterberg Limits LL (%)	PL (%)	PI (%)	CF (%)	Activity	USCS	I_R (G_{max})
Natural	Atchafalaya	102	40	62	82	0.76	CH	218
	Troll	54	24	30	-	-	CH	734
	BBC	48	20	28	56	0.50	CL	536
	Onsøy	67	24	43	69	0.62	CH	273
Manufac-tured	PureGold Gel	394	27	367	89	4.12	CH	46
	Kaolinite	67	35	32	57	0.56	MH	358

Note: clay fraction = % < 0.002 mm, Activity = PI/clay fraction, I_R values from Fig. 4

Fall Cone Testing

Evolution of the undrained shear strength during thixotropic hardening was measured using the fall cone (FC) device as per ISO 17892-6 (2017) using a 60˚/60 g cone. Specimens were prepared for testing by placing thoroughly remolded soil into a series of glass jars (Fisher Scientific, Inc.) with an inner diameter of 45 mm and an inner height of 44 mm. The soil was systematically placed inside the jars with a spatula to avoid trapping air. The top surface of the specimens was smoothed flush with the top of the jar mouth also using a spatula and sharp knife. To maintain constant water content, the jars were sealed using a layer of vacuum grease and a thin sheet of parafilm placed between the soil and the inside surface of the jar caps. Additionally, the sealed jars were stored underwater in a temperature control box set at 24° C. The specimens were typically tested at 0, 1, 2, 4, 8, 16, 32, and 64 days. For each test specimen, once the jar was opened and the top surface of the specimen exposed, three to five FC measurements were obtained at different locations. These values were averaged and s_u was computed as (ISO 2017)

$$s_u = (cmg)/i^2 \quad [1]$$

where c = constant determined by the tip angle of the cone = 0.27 for a 60˚ cone; g = gravitational acceleration at free fall (i.e., 9.81 m/s^2); m = mass of the cone = 60 g; i = the cone penetration (in mm) into the specimen. For quality control, once the fall cone measurements were conducted selected specimens were again fully remolded to ensure that s_u was equal to the t = 0 value. Furthermore, once fall cone testing was completed, the water content of the cured specimen was measured and compared to the t = 0 value.

Bender Element Measurements

Specimens prepared for bender element testing were selected from the same batch of soil prepared for the fall cone specimens. The soil was placed in a 100 mm tall by 63 mm inside diameter acrylic container machined with inside lips that accommodated top and bottom platens (Fig. 1). The container was sealed at the platen connections with vacuum grease, parafilm, and electrical tape. Since use of the bender elements was a non-destructive measurement method, only one specimen was needed for each clay and multiple measurements were possible during the full thixotropic hardening period. Once prepared, each specimen was placed in a temperature-controlled box at 24 ˚C during the thixotropic process.

The top and bottom platens each contained a central bender element that was either directly epoxied into the platen (Landon et al. 2007) or housed in a stainless steel mounting disc that was epoxied into the platen (Salazar and Coffman, 2014). Parallel and series poled piezoceramic elements were used as transmitting and receiving elements, respectively. Each element was waterproofed using epoxy, electronically grounded, and calibrated to determine calibration time and orientation of platens to ensure positive wave polarization between the transmitter and receiver. The transmitting signal was generated by a Wavetek model 29 10 MHz Direct Digital Synthesis (DDS) Function Generator. The function generator was used to excite the transmitting bender with a single ±10 V amplitude sine wave triggered at a 10 Hz delay. The excitation frequency was selected such that the received signal nominally matched the excitation frequency (e.g., ASTM 2020) and for the clays tested in this work ranged from 0.5 to 2.0 kHz. The transmitted and received signals were both recorded using a Pico PC-based oscilloscope (Model 5242B) with variable 12 bit or 16 bit resolution and PicoScope 6 software. The received traces were averaged over time and a 30 kHz low-pass filter was applied using PicoScope 6. The filter did not change the arrival signal sufficiently to measurably alter the travel times of the shear waves.

The vertically propagating, horizontally polarized shear wave velocity V_{vh} was calculated as

$$V_{vh} = L_{tt}/(\Delta_t - t_c) \qquad [2]$$

where L_{tt} = tip-to-tip distance between the bender elements; t_c = calibration time; Δt = shear wave travel time which was estimated using the first zero crossover method (Kawaguchi et al. 2001; ASTM 2020). Due to near field effects there was often a slight negative deviation in the received wave prior to the arrival of the wave. The first zero crossover was determined by fitting a horizontal line to the pre-deviation received wave and extending that line until it first intersected with the post-deviation received wave. The small-strain shear modulus G_{max} was computed as

$$G_{max} = \rho_t(V_{vh})^2 \qquad [3]$$

where ρ_t = total density.

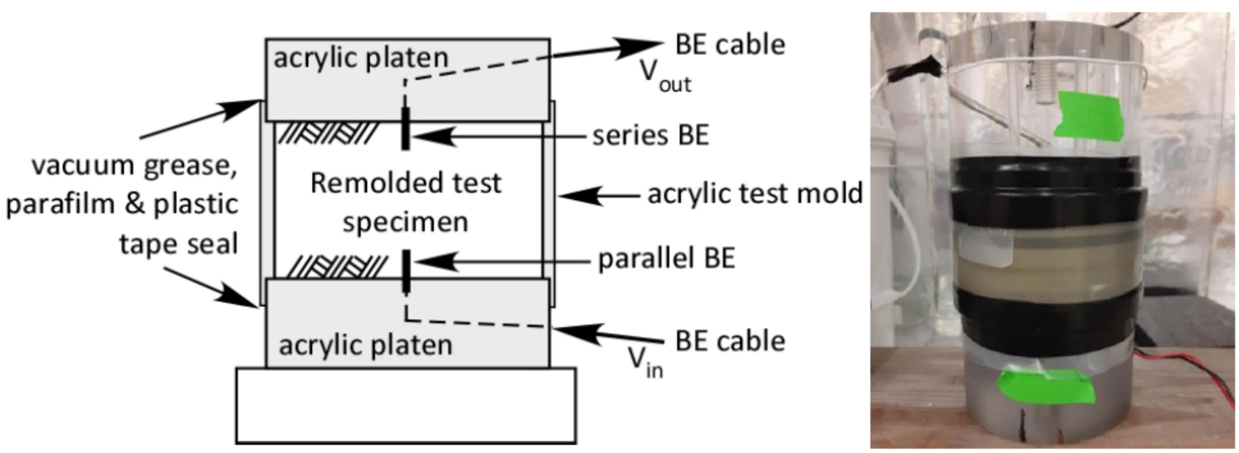

Fig. 1. (a) Schematic of thixotropy test container with bender element platens, and b) photo.

RESULTS AND DISCUSSION

Fall cone and Bender Element Measurements

Figure 2a plots the fall cone s_u versus thixotropic curing times with s_{u0}, defined as s_u at $t = 0$ days, ranging from 1.1 to 4.4 kPa. Thereafter, all the clays exhibit thixotropic hardening to various extents, although all generally have an initial significant increase in s_u during the first few days followed by a decrease in the rate of increase in s_u with time. Since the clays all had different s_{u0} values, Figure 2b plots thixotropy strength ratio s_u/s_{u0} as defined by Yang and Andersen (2016). These results show that at around $t = 32$ days all the clays have a thixotropy strength ratio of at least 2.0 and as high as 3.5. Various equations were used to fit the temporal data with the best performing equation being a version of Burgers' five parameter material model (Barnes 2000)

$$s_u = c_1 + c_2(1 - exp(c_3t)) + c_4(1 - exp(c_5t)) \quad [4]$$

where c_1 to c_5 are the optimized fitting parameters. The dashed lines in Figure 2 represent the best fit form of Equation 4 for each clay.

Each test specimen's water content was measured to verify that it did not change during the thixotropic curing period. The measurements showed very little variation in water content with the following statistics for each clay: 1) BBC average value of all specimens $\bar{x}$ = 45%, standard deviation s = 0.39, coefficient of variation CV = 0.87%; 2) Troll, $\bar{x}$ = 54%, s = 0.14, CV = 0.25%; 3) Pure Gold Gel $\bar{x}$ = 418%, s = 4.0, CV = 0.95%; 4) Kaolin $\bar{x}$ = 58%, s = 0.64, CV = 1.1%; 5) Atchafalaya, $\bar{x}$ = 93%, s = 1.6 and CV = 1.7%; and 6) Onsøy, $\bar{x}$ = 66%, s = 0.51 and CV = 0.77%.

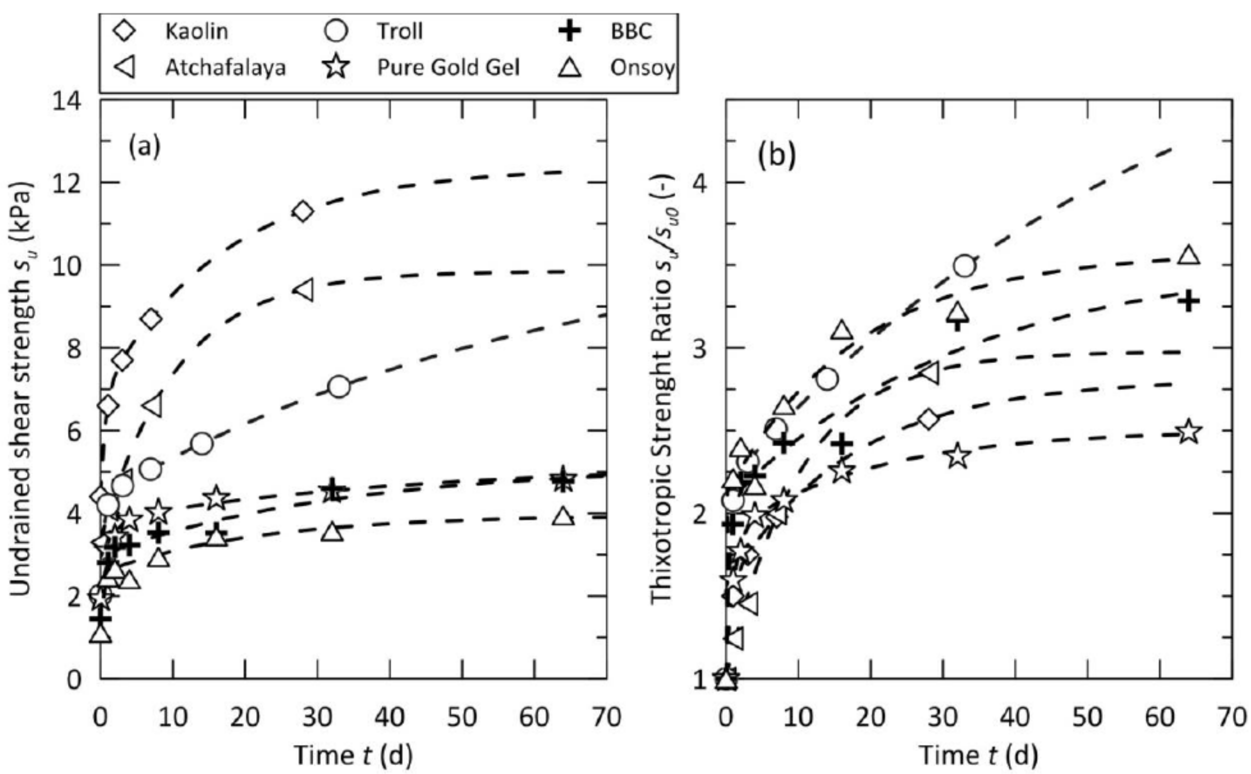

Fig. 2. (a) Fall cone undrained shear strength versus time and (b) thixotropic strength ratio s_u/s_{u0} versus time

Figure 3a plots V_{vh} determined by the bender elements for the six clay samples versus time and Figure 3b plots the data normalized by V_{vh} at t = 0 days. Since for these tests the measurements were non-destructive many more data points were collected. As per the fall cone s_u behavior, V_{vh} and V_{vh}/V_{vh0} also increase with time in nominally two stages and show very similar time-dependent behavior, i.e., the shape of the curves and the location of the apparent inflection points. At around t = 32 days all the clays have a thixotropy shear wave velocity ratio V_{vh}/V_{vh0} ranging from 1.4 to 2.3. The dashed lines represent the best fit Equation 4 to the data. For these six clays there is a general trend of decease in both the thixotropic strength ratio and the thixotropic shear wave velocity ratio with an increase in liquid limit.

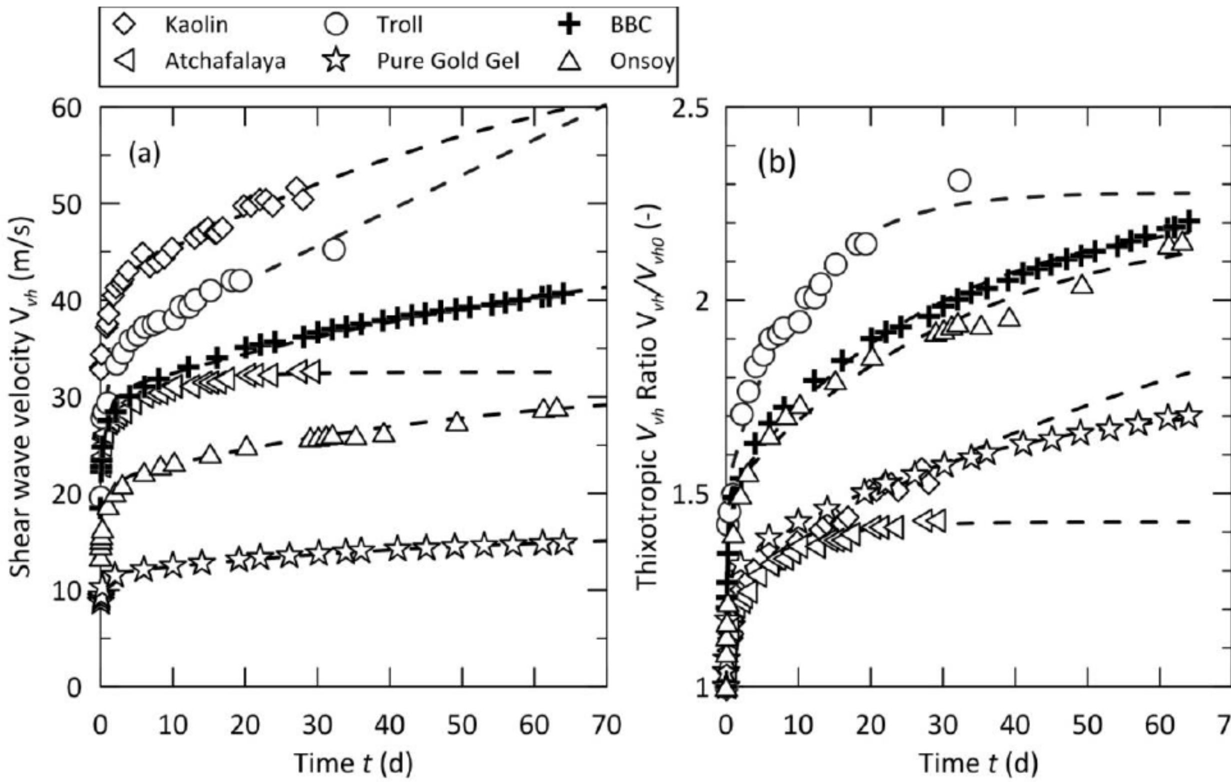

Fig. 3. (a) Bender element shear wave velocity data versus time, and b) thixotropic shear wave velocity ratio V_{vh}/V_{vh0} versus time

Rigidity Index Data

Figure 4a plots G_{max} versus s_u for bender element V_{vh} and fall cone s_u data measured at the same curing time. Collectively the dataset for the six clays suggests that I_R remains approximately constant during the thixotropic curing period. Accordingly, also plotted with dashed lines in Figure 4a are results of linear regression (with zero intercept) for each clay. The corresponding I_R values are also included in the figure and listed in Table 1. Figure 4b plots these values versus plasticity index except for the very high PI Pure Gold Gel that also has the lowest I_R value. Figure 4b plots the empirical correlation by Keaveny and Mitchell (1986) and Mayne (2007) among I_R, OCR, and PI as follows:

$$I_R \approx [exp(0.0435(137 - PI))]/[1 + ln\{1 + 0.0385(OCR - 1)^{3.2}\}]^{0.8} \qquad [5]$$

where OCR = σ'_p/σ'_{v0}, overconsolidation ratio. The OCR for Equation 5 was set equal to one for the line plotted in Figure 4b. Although, while the fully remolded soils can reasonably be assumed to have started at a normally consolidated state, in reality thixotropic hardening can be considered as a preconsolidation mechanism and the apparent OCR of the test specimens likely increased during the curing process. The Equation 5 I_R values are based on G_{50} (i.e., G_{50}/s_u) and thus not surprisingly I_R values for the six remolded clays based in G_{max} are much higher. The Equation 5 empirical correlation shows an exponential type decrease in I_R (based on G_{50}) with increasing PI. Similarly, the I_R (based on G_{max}) versus PI data for the six remolded clays also suggest an exponential type of decrease with increasing PI.

Krage et al. (2014) compiled a database of I_R values for eight soft clays of varying *PI* with G_{max} from downhole seismic piezocone or from bender element measurements from CAUC test specimens together with values of G_{50} and s_u from the monotonic CAUC tests. The resulting ratio G_{50}/G_{max} was found to be approximately constant, equal to an average value of 0.26, independent of OCR. While recognizing that the Krage et al. (2014) database was created using CAUC test data conducted on good-quality intact samples, it is of interest to note that, if the 0.26 factor is applied to the I_R values of the six remolded specimens, the resulting data plot on and around the empirical relationship depicted by Equation 5.

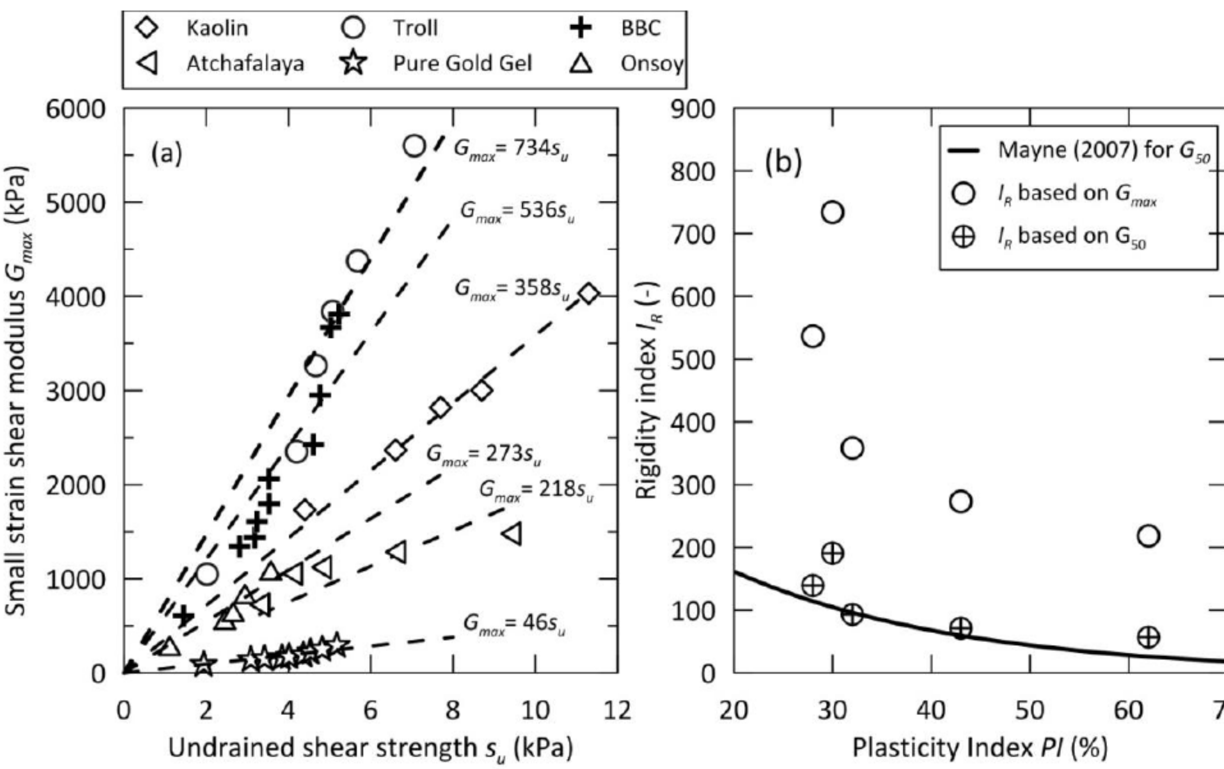

Fig. 4. (a) G_{max} versus s_u at different thixotropic curing times, b) Rigidity Index versus plasticity index (excluding Pure Gold Gel with I_R for G_{max} = 45 at *PI* = 367%)

CONCLUSIONS

This paper presents results from a set of experiments that measured the evolution of fall cone undrained shear strength s_u and bender element shear wave velocity V_{vh} of six fully remolded soft clays of varying plasticity during thixotropic hardening. In all cases the clays exhibited a significant temporal gain in both s_u and V_{vh} with the greatest increase occurring during the initial 2 to 4 days. The thixotropic strength ratio s_u/s_{u0} at around 32 days ranged between 2.0 and 3.5 while the thixotropic shear wave velocity ratio V_{vh}/V_{vh0} ranged from 1.4 to 2.3. The evolution of both s_u and V_{vh} with time is well modeled by Burgers' five-parameter material model. For the six clays there is a general trend of decease in both the thixotropic strength ratio and the thixotropic shear wave velocity ratio with an increase in liquid limit or plasticity index. For all clays the rigidity index I_R, taken as the ratio of the small-strain shear modulus to undrained shear strength G_{max}/s_u, computed using V_{vh} (to compute G_{max}) and fall cone s_u data measured at the same curing time, is approximately constant during the thixotropic curing period. The I_R values generally decrease with an increase in liquid limit or plasticity index. If the bender element G_{max} values are reduced to G_{50} using the empirical correlation of Krage et al. (2014) the resulting I_R values are similar to that of the empirical correlation presented by Mayne (2007) for intact clays and with an assumed overconsolidation ratio equal to one. These results suggest similar I_R values whether the clay is intact or fully remolded. Additional testing is required to further validate this preliminary finding, ideally from a test program consisting of companion CAUC type testing with bender elements on both high-quality intact samples and thixotropically cured, fully remolded samples of the same clays.

ACKNOWLEDGMENTS

This work was supported in part by the National Science Foundation (NSF) under grant CMMI 1640306. Any opinions, findings, and conclusions or recommendations expressed in this paper are those of the authors and do not necessarily reflect the views of the NSF.

REFERENCES

American Society for Testing and Materials - ASTM (2020).*Volume 04.08 - Soil and Rock (I): D420 to D5876 and Volume 04.09 - Soil and Rock (II): D5877 to latest*. ASTM International, West Conshohocken, PA, USA.

Andersen, K.H., Jostad, H.P., 2004. Shear Strength Along Inside of Suction Anchor Skirt Wall in Clay. Offshore Technol. Conf. https://doi.org/10.4043/16844-MS

Andersen, K.H., Jostad, H.P., 2002. Shear Strength Along Outside Wall of Suction Anchors in Clay after Installation, in: The Twelfth International Offshore and Polar Engineering Conference. International Society of Offshore and Polar Engineers, Kitakyushu, Japan.

Arnold, J.E., Goodeve, C.F., 1940. The Coefficient of Thixotropy of Suspensions of Carbon Black in Mineral Oil. J. Phys. Chem. 44, 652–670. https://doi.org/10.1021/j150401a013.

Barnes, H.A. 2000. A Handbook of Elementary Rheology. Institute of Non-Newtonian Fluid Mechanics, University of Wales, Aberystwyth.

Chang, C., Nguyen, Q.D., Rønningsen, H.P., 1999. Isothermal start-up of pipeline transporting waxy crude oil. J. Nonnewton. Fluid Mech. 87, 127–154. https://doi.org/10.1016/S0377-0257(99)00059-2.

DeJong, J.T., Randolph, M.F. 2012. Influence of Partial Consolidation during Cone Penetration on Estimated Soil Behavior Type and Pore Pressure Dissipation Measurements. *Journal of Geotechnical and Geoenvironmental Engineering*, Vol. 138, No. 7, 777-788.

Gamble, D.L., 1936. THIXOTROPY IN PAINTS Influence on Packaging and Application Properties of Flat Wall Coatings. Ind. Eng. Chem. 28, 1204–1210. https://doi.org/10.1021/ie50322a020

ISO 17892-12, 2018. Geotechnical investigation and testing - Laboratory testing of soil - Part 12: Determination of Atterberg limits.

ISO/TS 17892-6, 2017. Geotechnical investigation and testing - Laboratory testing of soil - Part 6: Fall cone test.

Kawaguchi, T., Mitachi, T., Shibuya, S. 2001. Evaluation of shear wave travel time in laboratory bender element test. *Proc., 15th Int. Conf. on Soil Mechanics and Geotechnical Engineering*, ISCGME, Vol. 1, 155–158.

Keaveny, J.M., Mitchell, J.K., 1986. Strength of fine-grained soils using the piezocone, in: Use of In Situ Tests in Geotechnical Engineering. ASCE, Reston, Virginia, pp. 668–685.

Krage, C.P., Broussard, N.S., DeJong, J.T., 2014. Estimating rigidity index based on CPT measurements, in: Third International Symposium on Cone Penetration Testing. Las Vegas, Nevada, USA, pp. 727–735.

Landon, M.M., DeGroot, D.J., Sheahan, T.C. 2007. Non-Destructive sample quality assessment of a soft clay using shear wave velocity. *J. of Geotechnical and Geoenvironmental Eng.*, 133(4): 424-432.

Low, H.E., Lunne, T., Andersen, K.H., Sjursen, M.A., Li, X. Randolph, M.F. 2010. Estimation of intact and remoulded undrained shear strengths from penetration tests in soft clays. Geotéchnique, 60(11): 843-859.

Lunne, T., Andersen, K.H., 2007. Soft Clay Shear Strength Parameters For Deepwater Geotechnical Design, in: Proc., 6th Int. Offshore Site Investigation and Geotechnics Conf.: Confronting New Challenges and Sharing Knowledge. London. UK.

Ma, S., Qian, Y., Kawashima, S., 2018. Experimental and modeling study on the non-linear structural build-up of fresh cement pastes incorporating viscosity modifying admixtures. Cem. Concr. Res. 108, 1–9. https://doi.org/10.1016/J.CEMCONRES.2018.02.022

Mayne, P.W., 2007. Cone penetration testing state-of-practice. NCHRP Proj. 20–05.

Mitchell, J.K., 1960. Fundamental Aspects Of Thixotropy In Soils. Soil Mech. Found. Div. 86, 19–52.

Mitchell, J.K., Soga, K., 2005. Fundamentals of Soil Behavior, John Wiley & Sons Inc. Hoboken, NJ. https://doi.org/10.1016/j.jhazmat.2005.06.004

Moretto, O., 1948. Effect of Natural Hardening on the Unconfined Compression Strength of Remolded Clays, in: Proc., 2nd Int. Conf. on Soil Mechanics and Foundation Engineering. Rotterdam, pp. 137–144.

Randolph, M., Cassidy, M., Gourvenec, S., Erbrich, C. 2013. Challenges of offshore geotechnical engineering. Proc. 16th Int. Conf. Soil Mechanics and Geot. Eng., Osaka, Japan.

Salazar, S.E., Coffman, R.A. 2014. Design and Fabrication of End Platens for Acquisition of Small-Strain Piezoelectric Measurements During Large-Strain Triaxial Extension and Triaxial Compression Testing, *Geotechnical Testing Journal*, 37(6),

Seng, S., Tanaka, H., 2012. Properties of very soft clays: A study of thixotropic hardening and behavior under low consolidation pressure. Soils Found. 52, 335–345. https://doi.org/10.1016/J.SANDF.2012.02.010

Skempton, A.W., Northey, R.D., 1952. The Sensitivity of Clays. Géotechnique 3, 30–53. https://doi.org/10.1680/geot.1952.3.1.30

Teh, C.I., Houlsby, G.T., 1991. An analytical study of the cone penetration test in clay. Géotechnique 41, 17–34. https://doi.org/10.1680/geot.1991.41.1.17

Turner, A.J., Rodewald, C.W., 1949. An experimental study of thixotropy in bentonite suspensions. J. Colloid Sci. 4, 283–298. https://doi.org/10.1016/0095-8522(49)90010-0

Vesic, A.S., 1972. Expansion of cavities in infinite soil mass. Soil Mech. Found. Div. 98, 265–290.

Yang, S., Andersen, K.H., 2016. Thixotropy of Marine Clays. Geotech. Test. J. 39. https://doi.org/10.1520/GTJ20150020

Zhang, G., Yin, H., DeGroot, D.J., 2013. Thixotropism of micron-sized saltwater clay flocs. Géotechnique Lett. 3, 162–165. https://doi.org/10.1680/geolett.13.00049

Zhang, X.W., Kong, L.W., Yang, A.W., Sayem, H.M., 2017. Thixotropic mechanism of clay: A microstructural investigation. Soils Found. 57, 23–35. doi.org/10.1016/j.sandf.2017.01.002.